ELSEVIER

Surface Science 412/413 (1998) 645–656

surface science

Equilibrium fluctuations and decay of step bumps on vicinal Cu (111) surfaces

Margret Giesen *, Georg Schulze Icking-Konert

Institut für Grenzflächenforschung und Vakuumphysik, Forschungszentrum Jülich, D-52425 Jülich, Germany

Received 4 February 1998; received in revised form 29 May 1998

Abstract

Using scanning tunneling microscopy we have investigated the time dependence of equilibrium step fluctuations and the time dependence of the decay of bumps in (100) steps on Cu (111) vicinal surfaces. From the analysis of the equilibrium fluctuations we find that the dominant mass transport is along the step edges with an activation energy for diffusion along a kinked step of 0.37 eV. Using this result we estimate an upper limit for the hopping barrier along (100) steps to be 0.24 eV. Non-equilibrium bumps in steps occur when wandering monatomic islands attach to a step edge. We have analyzed the time dependence of the decay of these bumps. From the Fourier representation of the bump decay we find that the dependence of the time constant on the wave number q is that of a q^{-4} law. This result is consistent with the analysis of the equilibrium fluctuations.

Keywords: Copper; Diffusion and migration; Equilibrium thermodynamics and statistical mechanics; Non-equilibrium thermodynamics and statistical mechanics; Scanning tunneling microscopy; Single crystal surfaces; Surface defects; Vicinal single crystal surfaces

1. Introduction

The investigation of equilibrium step fluctuations and mass transport kinetics by scanning tunneling microscopy (STM) has become a powerful tool for studies of diffusion processes on surfaces in UHV [1–11] and in contact with a liquid [12]. The development of experimental and theoretical techniques, and of sophisticated computer codes has provided new and exciting information about the dynamics of equilibrium step fluctuations, island diffusion [13], ripening of nucleated islands [14–18], and the nature of the diffusion processes involved. The combination of theoretical and experimental work has allowed a large set of activation energies and pre-exponential factors, kink formation energies and step energies to be extracted from STM data.

In this work we analyze the equilibrium step fluctuations to study diffusion processes on copper (111) vicinal surfaces. We measured the time dependence of the mean square deviation in step positions along (100) steps. The time dependence obeys a $t^{1/4}$ law, indicative of mass transport along steps. From a temperature-dependent measurement we determine the activation energy of the step fluctuations. Information about the mass transport can also be extracted from the analysis of the decay of non-equilibrium step profiles. From the time dependence of the Fourier components of the non-equilibrium profile one can determine the dominant type of mass transport involved in the

* Corresponding author. E-mail: m.giesen@fz-juelich.de

0039-6028/98/$ – see front matter
PII: S0039-6028(98)00499-3

decay. In this work we have measured the decay of a bump on Cu (111) and we will show that the quantitative analysis of the non-equilibrium situation is in agreement with the analysis of the equilibrium step fluctuations.

Concern has been raised about a possible influence of the tunneling tip on the quantitative results obtained by STM measurements [19–21]. Nevertheless, the STM is appropriate for the investigation of surface dynamic processes, provided the experimentalists use high enough values for the tunneling resistance which have to be adapted to the system studied [20,21]. Here, we will show that for typical tunneling parameters the quantitative results on Cu (111) are not influenced by the tunneling probe.

The paper is organized as follows: In Section 2, we briefly discuss the basic theory used for the analysis of the experimental data. We also describe the experimental set-up and the sample preparation method. In Section 3, we present the experimental results on the equilibrium step fluctuations. Subsequently, the results obtained from a non-equilibrium experiment are shown. The paper concludes with a discussion of all results in terms of diffusion energies in Section 4 and a brief summary in Section 5.

2. Theoretical analysis and experimental set-up

The theory for the decay of non-equilibrium shapes was originally developed for two-dimensional periodic sinusoidal profiles on surfaces [22]. This theory can be applied to the analogous one-dimensional problem of the decay of local protrusions, so called bumps in step edges. The time dependence of the bump decay is correlated with the mass transport involved. The application of this concept to *equilibrium* step fluctuations is based on the assumption that fluctuations in the step edge position can be interpreted as small local bumps in the step edge. The time dependence of equilibrium step fluctuations is analyzed by means of a time-dependent correlation function which is defined as the mean square difference between step positions. The time correlation function obeys a power law with the exponent depending on the type of mass transport involved. The probably most straightforward presentation of the theory is in a paper of Pimpinelli et al. which considers all relevant cases [23]. We refer to this work for a detailed description of the different time laws. A brief overview is also given in Ref. [12]. In the following we briefly discuss the theoretical equations for the correlation function for the two cases relevant to this work.

2.1. Time correlation function in equilibrium

When the mass transport is restricted to the step edges the time dependence of the step edge position is given by the Langevin equation [22,24]

$$\frac{\partial x}{\partial t} = -\Omega \frac{\tilde{\beta}}{k_B T} D_{st} \frac{\partial^4 x}{\partial y^4} \tag{1}$$

Here, x denotes the direction perpendicular to the step edge and y the direction along the step. $\tilde{\beta}$ is the step edge stiffness [25]. The area Ω of an atom is given by $\Omega = a_\perp a_\parallel$ where $a_\perp$ and $a_\parallel$ are the atomic distances in the x- and y-directions, respectively[1]. The mean diffusion coefficient for mass transport along the steps, D_{st}, can be written in terms of the product of the tracer diffusion coefficient D_{tr} and the adatom concentration c_{st} per atom at the step edge, as long as $c_{st} \ll 1$:

$$D_{st} = a_\parallel c_{st} D_{tr} \quad \text{for } c_{st} \ll 1 \tag{2}$$

We note that the tracer diffusion coefficient involves hopping processes along a straight step and over kink sites. The step edge stiffness $\tilde{\beta}$ is related to the diffusivity b^2 by [25]

$$b^2 = \frac{k_B T}{\tilde{\beta}} a_\parallel \tag{3}$$

For low temperatures, the diffusivity can be expressed by the kink concentration P_k [25]

$$b^2 \approx P_k a_\perp^2 \approx 2e^{-(\epsilon/k_B T)} a_\perp^2 \quad \text{for } k_B T \ll \epsilon \tag{4}$$

where ϵ is the kink formation energy. Using

[1] For steps on Cu (111) along the dense [1$\bar{1}$0] direction $a_\perp$ and $a_\parallel$ are equal to 2.21 Å and 2.55 Å, respectively.

Eqs. (3) and (4), Eq. (1) becomes

$$\frac{\partial x}{\partial t} \approx -\frac{a_{\parallel}^3}{P_k} D_{st} \frac{\partial^4 x}{\partial y^4} \tag{5}$$

To convert Eq. (5) into atomic units we define

$$\hat{x} = \frac{x}{a_{\perp}}, \quad \hat{y} = \frac{y}{a_{\parallel}} \tag{6}$$

Then, Eq. (5) becomes

$$\frac{\partial \hat{x}}{\partial t} = -\frac{1}{P_k} \hat{D}_{st} \frac{\partial^4 \hat{x}}{\partial \hat{y}^4} \tag{7}$$

with $\hat{D}_{st} = D_{st}/a_{\parallel}$.

In order to study equilibrium fluctuations a noise term is added to Eq. (7) and the equation is solved for the correlation function [24]:

$$\hat{F}(t) = \langle [\hat{x}(t, \hat{y}_0) - \hat{x}(0, \hat{y}_0)]^2 \rangle \tag{8}$$

where the coordinate $\hat{y}$ parallel to the step edges is held constant at $\hat{y}_0$.

In the case of mass transport along the step edges $\hat{F}(t)$ is [10,23,24]

$$\hat{F}(t) \approx 0.464 P_k^{3/4} (\hat{D}_{st})^{1/4}\ t^{1/4} \tag{9}$$

Here, we use the expression given in Ref. [24] because it represents the solution for equilibrium fluctuations. A $t^{1/4}$ law is also obtained in another case when mass is exchanged with the terraces in the presence of a large step edge barrier. Atoms detached from the step edge cannot cross the adjacent descending step which has a distance $\hat{L}$ (in atomic units) and are reflected onto the terrace. In this case, $\hat{F}(t)$ is given by [23]

$$\hat{F}(t) \approx P_k^{3/4} (\hat{D}_s)^{1/4} \hat{L}^{1/4} t^{1/4} \tag{10}$$

with $\hat{D}_s$ the mean diffusion coefficient on the terrace in atomic units. Eqs. (9) and (10) can be rewritten as

$$\hat{F}(t) = c_{\delta}(T) \hat{L}^{\delta} t^{1/4} \quad \text{with } \delta = 0 \text{ or } 1/4 \tag{11}$$

The temperature-dependent pre-factors $c_0(T)$ and $c_{1/4}(T)$ are different for the two mass transport situations.

2.2. Time correlation function in a non-equilibrium situation

For the analysis of the time dependence for the bump decay it is more convenient to use the Fourier representation of Eq. (1). Then, the time correlation function is given by [26]

$$\hat{G}_{\hat{q}}(t - t_0) = \langle |\hat{x}_{\hat{q}}(t) - \hat{x}_{\hat{q}}(t_0)|^2 \rangle = A(T) \left[1 - \exp\left(-\frac{t - t_0}{\tau_{\hat{q}}} \right) \right] \tag{12}$$

in which $A(T)$ is the temperature-dependent amplitude of the Fourier components. The time constant $\tau_{\hat{q}}$ depends on the wave number of the Fourier component. In the following, we only need the expression of the diffusion coefficient as a function of the wave number $\hat{q}$ where $\hat{q}$ is given in atomic units ($\hat{q} = q/a_{\parallel}$). Solving Eq. (7) by the ansatz

$$\hat{x} = \exp[-(t/\tau_{\hat{q}})] \exp(i\hat{q}\hat{y}) \tag{13}$$

yields:

$$\tau_{\hat{q}} = \frac{P_k}{\hat{D}_{st} \hat{q}^4} \tag{14}$$

The $\hat{q}^{-4}$ dependence of the time constant $\tau_{\hat{q}}$ is characteristic for the case of atomic motion alongside the step edge [24].

We note that the application of Eq. (7) to the situation of the non-equilibrium decay of a bump is not a priori justified. For the derivation of Eq. (7) it is assumed that the step curvature is small. In the case of our experiments this assumption is reasonably fulfilled. In particular, it turns out that the flux along the step periphery, which is the important quantity in our analysis, is nearly unaffected by this approximation even for relatively large distortions perpendicular to the step edges as analyzed in this work.

2.3. Experimental set-up and sample preparation

The experiments were performed in a standard ultrahigh vacuum chamber with a base pressure of 5×10^{-11} mbar. Our temperature-variable scanning tunneling microscope is of the Besocke type. Typical tunneling parameters used during the

measurements are $I_T = 1.5$ nA and $U_T = +0.6$ V. The temperature of the sample during the STM measurements is changed by radiative cooling and heating.

The measurements of the step fluctuations were performed on (21 21 23) and (19 17 17) surfaces. The (21 21 23) surface is tilted with respect to the (111) plane along the $[11\bar{2}]$ direction. The angle is 2.49°. Hence the surface consists of parallel monatomic (100) steps along $[\bar{1}10]$ and the mean terrace width is 47.8 Å. A surface with indices (19 17 17) is obtained for a miscut angle of 3.05° along the same direction. Here, the mean distance between the (100) steps is 32.3 Å.

The samples were cut by spark erosion from a (111) copper single crystal bar. They were mechanically and electrochemically polished and oriented to the desired orientations by diffractometry to within 0.2°. Before mounting in the chamber, the crystals were annealed for 2 h in an H_2:Ar (1:25) atmosphere at 900°C. After this procedure the crystals are well oriented and largely free of usual contaminants such as sulfur and carbon. The final preparation was performed in situ by many cycles of Ne^+ sputtering (1.3 keV) and annealing to 700°C. This preparation was finished by one cycle of moderate sputtering with 0.6 keV and annealing to 400°C. After this procedure the concentration of contaminants on the surface is far below the Auger detection limit.

3. Results

3.1. Equilibrium step fluctuations

Fig. 1 shows STM images of Cu (21 21 23) and (19 17 17) at 310 K. The parallel steps run from top to bottom and the steps ascend from left to right. The scanning direction is perpendicular to the step edges. In contrast to normal STM images, the images shown in Fig. 1 are so-called "time images". In time images, a single line across the steps is scanned repetitively and displayed in the normal STM image format. Hence, the axis along the step edges is a time axis. Fluctuations in a time image correspond to a shift of the step position to the left or the right during the scanning process. The shift in step position appears in STM images as a sudden jumps in the step position between consecutive scan lines. The jumps are caused by the hopping of kinks in the time span between subsequent scan lines. This phenomenon ("frizziness") has been discussed in detail in other publications [6,27].

Fig. 2 shows the time correlation function $\hat{F}(t)$

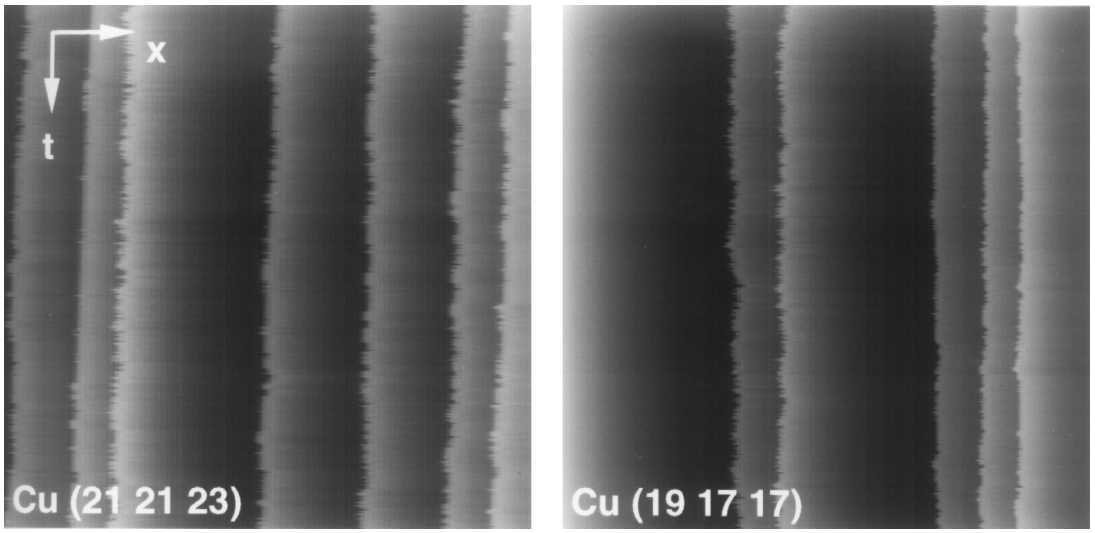

Fig. 1. Time images of Cu (21 21 23) and (19 17 17) at 310 K. The total time for each image is 45 s and the scan width is 194 nm.

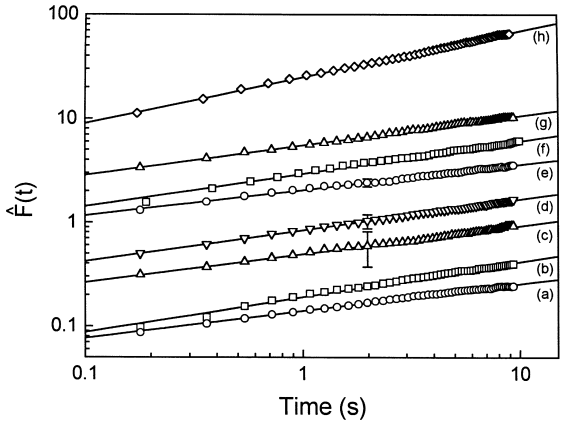

Fig. 2. Log–log plot of the time correlation functions on Cu (21 21 23) at different temperatures. The measured time exponents and the corresponding temperatures are indicated in Table 1.

Table 1
Measured time exponents of the correlation functions in Fig. 2. The error bars represent the statistical error of the linear fit

	T (K)	α
(a)	305	0.25 ± 0.01
(b)	325	0.32 ± 0.01
(c)	335	0.28 ± 0.01
(d)	363	0.30 ± 0.01
(e)	407	0.24 ± 0.01
(f)	440	0.30 ± 0.01
(g)	500	0.28 ± 0.01
(h)	600	0.45 ± 0.01

for Cu (21 21 23) for different temperatures. $\hat{F}(t)$ is well fitted by

$$\hat{F}(t)=c(T)t^{\alpha} \tag{15}$$

Here, $c(T)$ is temperature dependent and α is the time exponent which is indicative for the mass transport involved in the fluctuations. Table 1 shows the different exponents found at the various temperatures for the correlation functions plotted in Fig. 2. For temperatures below 500 K, α is close to 1/4. Only at the highest temperature in our experiment, $T=600$ K, did we find a value of $\alpha\approx1/2$. The error margins given in Table 1 reflect the statistical error obtained from the linear fit to the data. The true error is larger owing to systematic errors. A good estimate of the error is provided by counting the number of kinks passing a scan line in a distinct time span. In Fig. 2 we have plotted the error bars derived from the number of kinks for 335, 363 and 407 K. For low temperatures the error is relatively large since the kink concentration is small. For temperatures higher than 400 K, the error due to the number of kinks passing the scan line is already smaller than the statistical error given by the linear fit. It is reasonable to assume that the error margins determined from the number of kinks affect predominantly the absolute value of the correlation function and have a minor influence on the time exponent. Hence, one would expect the true error of the time exponent to be given by a value between the statistical error shown in Table 1 and the error determined from the number of kinks analyzed for each data point in the correlation functions as displayed in Fig. 2.

The temperature dependence of the pre-factor $c(T)$ (and hence of the time correlation function) in the lower temperature regime is that of an activated process, $c(T)\propto e^{-(E_t/k_BT)}$ In Fig. 3, $\hat{F}(2\text{ s})$ is plotted in an Arrhenius plot. The open and filled circles refer to data measured on the (21 21 23) and (19 17 17) surfaces, respectively. The data points are based on the analysis of the time correlation function for 60–140 steps. In addition, we have also plotted error bars for some of the data points. As described before, the error bars reflect the statistical error calculated from the

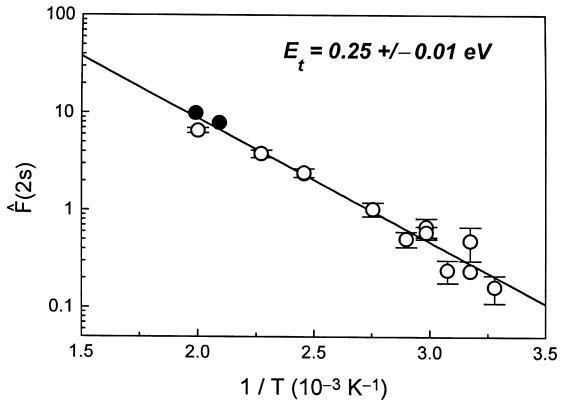

Fig. 3. Arrhenius plot of $\hat{F}(2\text{ s})$. The open and black circles refer to data measured on the (21 21 23) and the (19 17 17) surface, respectively.

total number of kinks which have passed the scan line in the time span up to $t=2$ s. For $T\leq 500$ K the activation energy is

$$E_t = 0.25 \pm 0.01 \text{ eV} \quad (16)$$

From the extrapolation of the linear fit to high temperatures, we obtain the value of $\hat{F}(2\text{ s})$ at $T\rightarrow\infty$:

$$\hat{F}(2\text{ s})|_{T\rightarrow\infty} = 3.05\times 10^{3\pm 0.19} \quad (17)$$

As we will discuss in Section 4, one can calculate the pre-exponential factor of the diffusion coefficient by means of Eq. (17).

We have also checked carefully for a possible influence of the tunneling tip on the analysis of the step fluctuations. We have measured the time correlation function $\hat{F}(t)$ as a function of the tunneling current and the bias while the temperature was held constant. Fig. 4(a) and 4(b) shows $\hat{F}(t)$ at 305 K for various tunneling resistances. In Fig. 4(a) the tunneling current has been held constant at $I_T=4.0$ nA and the bias U_T has been varied between $+0.3$ and $+1.2$ V. We have also plotted the statistical error arising from the total number of kinks which have passed the scan line at $t=2$ s and 9 s for the data set obtained at $U_T=+0.3$. The number of kinks increases with increasing time. Hence, the error margin is smaller for $t=9$ s compared with $t=2$ s. The error bars for the other data points are of the same order, but have not been plotted for simplicity. We have also checked for negative values of U_T and found no deviation from the curves in Fig. 4(a) within the error margins. Fig. 4(b) shows the correlation function at constant bias $U_T=+0.3$ V for different tunneling currents between $I_T=2.5$ nA and 4.0 nA. The error bars which have been determined as in Fig. 4(a) are plotted for $t=2$ s and 9 s for the data set at $I_T=2.5$ nA. In the panels of Fig. 4(a) and 4(b) it is obvious that the deviation in the absolute values of $\hat{F}(t)$ is well within the statistical error. Hence, a possible influence of the tunneling tip remains within the statistical error margins. Especially the measured time exponents are unaffected by a possible tip influence. We note that in particular no systematic dependence of $\hat{F}(t)$ on the tunneling resistance is observed. In case of tip-induced atomic motion along the steps one would

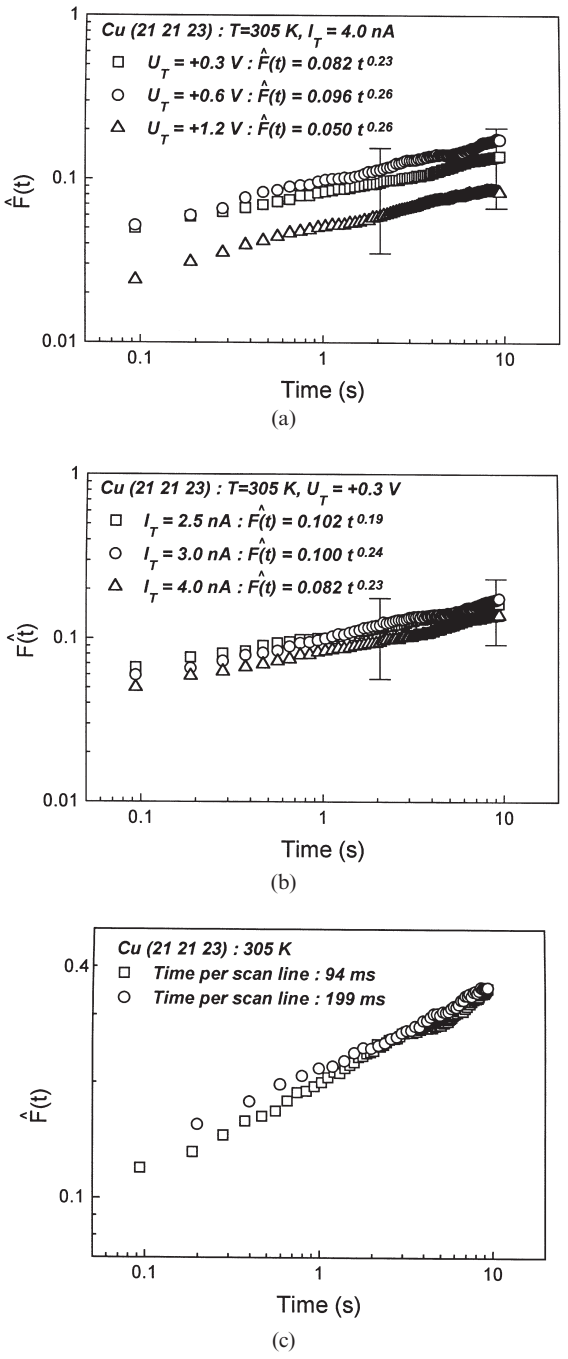

Fig. 4. $\hat{F}(t)$ measured (a) as a function of the tunneling bias for constant tunneling current and (b) as a function of the tunneling current for constant tunneling bias. (c) $\hat{F}(t)$ measured with two different scan times. The temperature was held constant at $T=305$ K.

expect $\hat{F}(t)$ to increase for decreasing tunneling resistance. This is not sustained by the measurements shown in Fig. 4(a) and 4(b).

A further means to check for a possible influence of the tunneling tip on $\hat{F}(t)$ is to change the scan time between consecutive scan lines. The total number of contacts between the tunneling tip and the step edge decreases with increasing time between two scan lines. Fig. 4(c) shows the time correlation function as a function of the time between two consecutive scan lines. The squares refer to data obtained at twice the scan speed compared with the data plotted as circles. Within the error margins both data sets reveal approximately the same time dependence of the step fluctuations. Therefore, we conclude that on Cu (111) surfaces there is no measurable tip influence on $\hat{F}(t)$ if moderate tunneling parameters are chosen in the experiment.

3.2. The dependence of the time correlation function on the terrace width

As remarked in Section 2.1, the $t^{1/4}$ law could arise from two different mass transport situations (Eqs. (9) and (10)). On Cu (111), a step edge barrier has been determined to be 0.12 eV [18]. Therefore, the transition from the exponent 1/4 to 1/2 found in the experimental data for increasing temperature could be interpreted in two different ways: One is that at low T the mass transport is restricted to the step edges ($\hat{F}(t) \propto t^{1/4}$ (Eq. (9)) and at higher temperatures atoms are exchanged with the terraces ($\hat{F}(t) \propto t^{1/2}$ [23,24]). The second possibility is that mass is exchanged with the terraces already at low temperatures, however, atoms cannot overcome the step edge barrier ($\hat{F}(t) \propto L^{1/4} t^{1/4}$ (Eq. (10)). Then, the transition to an exponent 1/2 above 500 K could mean that at this temperature a significant number of atoms are able to cross the barrier of an adjacent descending step ($\hat{F}(t) \propto L^{-1/2} t^{1/2}$ [23]).

In order to distinguish between the two possible cases we have measured $\hat{F}(t)$ as a function of the mean distance between adjacent steps. We have chosen STM data from surface areas with homogeneous step–step distances. The data was obtained from two different measurements on the (19 17 17) and the (21 21 23) surfaces at two different temperatures (478 and 503 K, respectively). From Eq. (11) it follows that (with $t = 2$ s)

$$\frac{\hat{F}(2\text{ s})}{(2\text{ s})^{1/4} c_\delta(T)} = \hat{L}^\delta \tag{18}$$

For the analysis, we have determined $c_\delta(T)$ from the common Arrhenius plot in Fig. 3. The results obtained from Eq. (18) are shown as circles in Fig. 5. The theoretical solutions for $\delta = 0$ and $\delta = 1/4$ are plotted as solid lines. These lines represent the expected distance dependence for the case of dominant mass transport along the step edges and for mass exchange with the terrace in presence of a large step edge barrier, respectively. Despite the scattering, the experimental data are much better described by the solution $\delta = 0$ compared with the prediction for $\delta = 1/4$. Hence, we conclude that below 500 K the dominant mass transport is along the step edges on Cu (111).

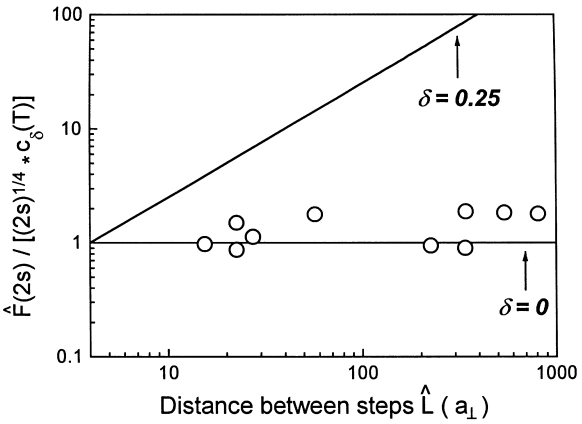

Fig. 5. Time correlation function as a function of the distance between adjacent steps. The solid lines $\delta = 0$ and $\delta = 0.25$ refer to the theoretical prediction when the mass transport is restricted to the step edges and when mass is exchanged with the terraces in the presence of a large step edge barrier, respectively.

3.3. Step fluctuations at non-equilibrium

Fig. 6 shows normal STM images of a Cu (111) surface after the deposition of a submonolayer amount of Cu on a gently sputtered surface at $T = 303$ K. Monatomic high, hexagonal islands

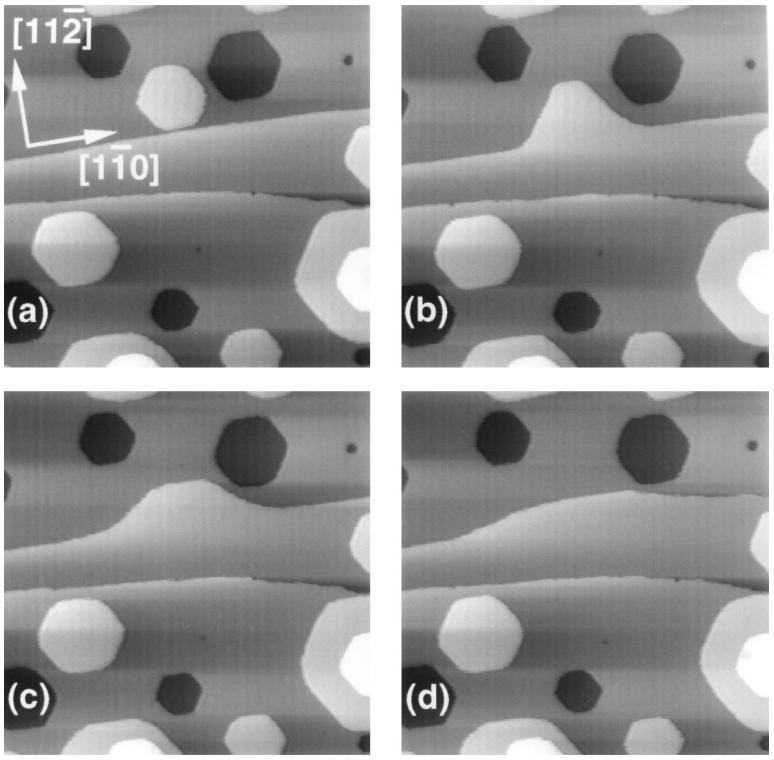

Fig. 6. (a) STM image of a monatomic island in close vicinity to a step edge at $T=303$ K. (b) The island suddenly attaches to the step edge and a bump occurs in the step profile. (c), (d) The bump decays in time owing to rapid edge diffusion along the step. The area shown in all images is 90 nm.

and vacancy islands have been formed on the terraces (Fig. 6(a)). These islands migrate on the surface owing to edge fluctuations and engage in a Brownian motion. The Brownian motion of monatomic vacancy islands has been investigated recently on Ag (111) by Morgenstern et al. [14]. Once in a while an island close to a step edge merges into the step. Then, a broad bump is formed in the step edge (Fig. 6(b)). The amplitude decreases and the bump becomes broader during time (Fig. 6(c) and 6(d)). Shortly after the island had merged into the step edge (Fig. 6(b)), the shape of the bump still reveals an approximately straight section along the [1$\bar{1}$0] direction resembling the nearly hexagonal shape of the islands. The shape of the islands is determined by the condition that the chemical potential around the periphery is constant. The edge segments of the islands are not straight but are rounded because the line tension has no cusp. In other words, the steps are always rough. As for the islands, the chemical potential along the periphery as well as the line tension and the curvature are continuously differentiable for the bump. We can analyze the time dependence of the bump decay by means of Eq. (1) [22].

In Fig. 7(a) the profile of the bump shown in Fig. 6 is plotted for different times. We have analyzed the Fourier components $\hat{q}$ of the profiles in Fig. 7(a). Fig. 7(b) shows the amplitude $A(\hat{q})$ of the Fourier components as a function of the time. For small values of $\hat{q}$ ($\hat{q}=0.025$ in Fig. 7(b)), one finds an exponential decay of the amplitude during the whole observation time. The solid line shows a least-squares fit to the data. For higher values of $\hat{q}$ ($\hat{q}=0.033$–0.058), the exponential decay is significant only for short times. In the long time limit, the noise in the Fourier analysis becomes greater than the measurable amplitude of the Fourier components. The noise is mostly due to

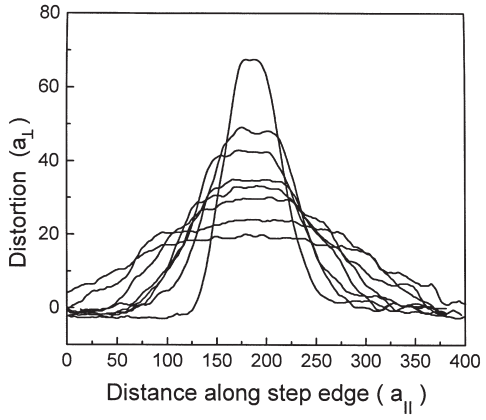

(a)

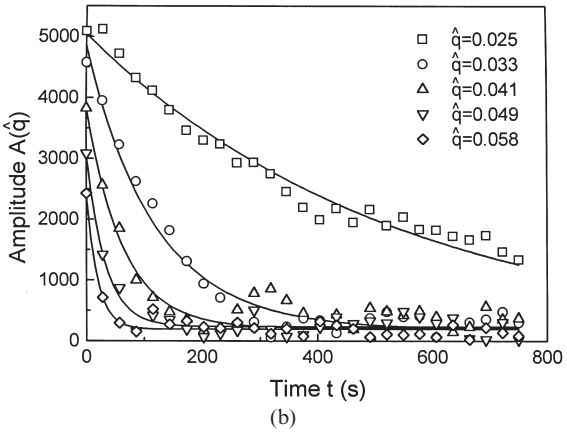

(b)

Fig. 7. (a) Step edge profile of the bump in Fig. 6 as a function of the time. (b) Amplitude of different Fourier components $\hat{q}$ as a function of time.

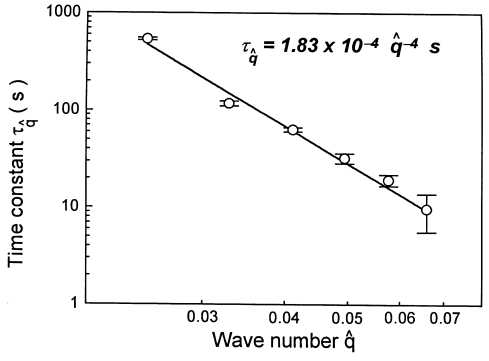

Fig. 8. Time constant $\tau_{\hat{q}}$ as a function of the wave number $\hat{q}$.

the error in the determination of the local step edge position and can be expressed by a constant contribution to the decay curves. In order to determine the time constant of the decay for low values of $\hat{q}$ we have therefore fitted the data by an exponential with a constant offset $A_0 = 205$ (solid lines). This offset has been determined by the average of the data for long times of all decay curves. From these fits we determine the time constants $\tau_{\hat{q}}$ (Eq. (12)). Fig. 8 shows $\tau_{\hat{q}}$ as a function of the wave number $\hat{q}$. We obtain

$$\tau_{\hat{q}} = (1.83 \pm 0.12) \times 10^{-4} \hat{q}^{-4} \text{ s} \tag{19}$$

4. Discussion

4.1. Equilibrium step fluctuations on Cu (21 21 23)

In the low temperature regime the time dependence of $\hat{F}(t)$ is that of a $t^{1/4}$ law (Fig. 2, Table 1). Since we measure no dependence of $\hat{F}(t)$ on the distance between steps (Fig. 5) we conclude that below 500 K the mass transport is restricted to the step edges.

Above 500 K $\hat{F}(t)$ approximately obeys a $t^{1/2}$ law which can be clearly distinguished from the time law in the low temperature regime. The measured exponent 1/2 could be evidence that terrace diffusion becomes dominant for higher temperatures. Since we obtained no data at temperatures higher than 600 K we restrict the discussion to the results obtained at temperatures below 500 K in the following.

First, we determine the diffusion coefficient $\hat{D}_{\text{st}}$ from the analysis of the equilibrium fluctuations. For that purpose we substitute $P_{\text{k}} = 2 \exp[-(\epsilon/k_{\text{B}}T)]$ in Eq. (9). With $\hat{D}_{\text{st}} = \hat{D}_0 \exp(-E_{\hat{D}_{\text{st}}}/k_{\text{B}}T)$ we rewrite Eq. (9) to:

$$\hat{F}(t) \approx 0.464 \hat{D}_0^{1/4} \exp[-(\tfrac{3}{4}\epsilon + \tfrac{1}{4}E_{\hat{D}_{\text{st}}})/k_{\text{B}}T] t^{1/4}$$

$$= \hat{F}(2\text{ s})|_{T\to\infty} \exp\left(-\frac{E_{\text{t}}}{k_{\text{B}}T}\right) t^{1/4} \tag{20}$$

The right-hand side of Eq. (20) describes the analytical form of the experimental correlation functions, where $\hat{F}(2\text{ s})|_{T\to\infty}$ denotes the y section of the extrapolated data in the Arrhenius plot in

Fig. 3. From Eq. (20) we obtain

$$\tfrac{3}{4}\epsilon + \tfrac{1}{4}E_{\hat{D}_{st}} = E_t, \quad 0.464\hat{D}_0^{1/4} = \hat{F}(2\ \mathrm{s})|_{T\to\infty} \tag{21}$$

A reasonable approximation for the kink formation energy ϵ is the value $\epsilon = 0.128$ eV measured on Cu (100) vicinal surfaces [6]. This value is in excellent agreement with calculations by Loisel et al. who determined $\epsilon = 0.129$ eV for both Cu (100) and Cu (111) surfaces [28]. Other authors calculate a lower value for ϵ, but agree that the kink energy should be about equal for Cu (100) and Cu (111) [29]. With $\epsilon = 0.128$ eV and Eqs. (16) and (17) one obtains

$$E_{\hat{D}_{st}} = 0.62 \pm 0.06\ \mathrm{eV} \tag{22}$$

and

$$\hat{D}_0 = 1.87 \times 10^{15\pm 2}\ \mathrm{s}^{-1} \tag{23}$$

One can compare the value of $\hat{D}_0$ with the typical pre-exponential factor for the diffusion of single atoms [30]

$$\hat{D}_0|_{\mathrm{theory}} \approx \frac{k_B T}{h} = 6.31 \times 10^{12}\ \mathrm{s}^{-1} \tag{24}$$

where we have used $T = 303$ K and h is the Planck constant. Considering the large error, the experimental value of $\hat{D}_0$ is in reasonable agreement with the theoretical value.

The activation energy of $\hat{D}_{st}$ contains the averaged diffusion energy along the steps E_{diff} as well as the formation energy E_{ad} of adatoms at the step edges (Eq. (2)). A reasonable estimation of E_{diff} is obtained assuming the formation energy of adatoms can be expressed in the nearest neighbor model in terms of the kink formation energy ϵ, $c_{st} = \exp(-2\epsilon/k_B T)$. Then, E_{diff} becomes

$$E_{diff} = E_{\hat{D}_{st}} - 2\epsilon = 0.37 \pm 0.06\ \mathrm{eV} \tag{25}$$

The activation barrier E_{diff} includes hopping over kink sites as well as along a straight step. The hopping energy E_d of adatoms along a straight step can be estimated using the theory of Natori and Godby [31]. According to [31] the tracer diffusion coefficient in Eq. (2) can be expressed in terms of microscopic hopping rates:

$$D_{tr} = \frac{n^2 \Gamma_d}{(n-1+1/S)(n-1+\Gamma_d/\Gamma_a)} \tag{26}$$

Here, the rates Γ_d, Γ_a and S are defined as

$$\begin{aligned} \Gamma_d &= \hat{D}_0\, e^{-(E_d/k_B T)} \\ \Gamma_a &= \Gamma_d\, e^{-(2\epsilon/k_B T)} \\ S &= e^{-(\Delta/k_B T)} \end{aligned} \tag{27}$$

E_d is the hopping barrier of adatoms along the step, ϵ is the kink energy and Δ is the additional barrier for hopping over a kink site. (Δ can be interpreted as a Ehrlich–Schwoebel barrier in one dimension, for details see also Ref. [32]). n is the distance between kinks in units of $a_\parallel$. At equilibrium, n is given by the inverse kink concentration:

$$n = \frac{1}{P_k} \approx \tfrac{1}{2} e^{\epsilon/k_B T} \tag{28}$$

With these notations and assuming that the kink concentration is small, Eq. (26) can be expressed as

$$D_{tr} = \frac{\hat{D}_0\, e^{-(E_d/k_B T)}}{2e^{\epsilon/k_B T} + 4e^{\Delta/k_B T}} \tag{29}$$

Then, from Eq. (2) it follows that

$$D_{st} = \frac{\hat{D}_0\, e^{-((2\epsilon + E_d)/k_B T)}}{2e^{\epsilon/k_B T} + 4e^{\Delta/k_B T}} \tag{30}$$

If the barrier for hopping over a kink site is smaller than the kink energy, $\epsilon \gg \Delta$, one has

$$3\epsilon + E_d \approx E_{\hat{D}_{st}} \tag{31}$$

With increasing value of the barrier Δ the energy calculated using Eq. (31) becomes smaller. Therefore, the calculated energy E_d represents an upper limit for the hopping barrier in the case $\epsilon \gg \Delta$. Using $\epsilon = 0.128$ eV and $E_{\hat{D}_{st}} = 0.62$ eV we find

$$E_d \le 0.24\ \mathrm{eV} \tag{32}$$

which is in excellent agreement with the calculated value 0.228 eV by Stoltze [29].

4.2. Time dependence at non-equilibrium

From the analysis of the time dependence of the bump decay we find that $\tau_{\hat{q}} \propto \hat{q}^{-4}$ (Eq. (19)). Both the equilibrium fluctuations and the decay of non-equilibrium profiles are therefore controlled by the mass transport along steps. Finally, we want to emphasize that the analysis of the bump decay is also in quantitative agreement with the analysis of the equilibrium fluctuations. We substitute $\hat{D}_{\mathrm{st}}$ in Eq. (9) by the expression in Eq. (14) and obtain

$$\hat{F}(t) \approx 0.464 P_{\mathrm{k}} \left(\frac{1}{\tau_{\hat{q}} \hat{q}^4} \right)^{1/4} t^{1/4} \tag{33}$$

Using $\tau_{\hat{q}} = (1.83 \pm 0.12) \times 10^{-4} \hat{q}^{-4}$ s (Eq. (19)), $\epsilon = 0.128$ eV and $t = 2$ s the expected value for $\hat{F}(2\ \mathrm{s})$ is

$$\hat{F}(2\ \mathrm{s}) = 0.1 \tag{34}$$

The experimental value of the correlation function at $T = 303$ K is $\hat{F}(2\ \mathrm{s}) = 0.2$. This value is in agreement with Eq. (34) within a factor within about 2. As we have already remarked in Section 3.1 this deviation is well within the statistical error of the time correlation function.

From a theoretical point of view the equivalence of the analysis of a bump decay and the analysis of the time dependence of equilibrium fluctuations is not surprising. Recently, Bartelt and Tromp showed the equivalence between the analysis of steps in equilibrium and non-equilibrium on Si (100) at high temperatures [33]. While these authors studied the equilibration of step edge profiles after rapid heating and subsequent cooling of the sample, we showed for the first time the equivalence on a metal surface keeping the temperature constant.

5. Summary

We have shown that on Cu (111) surfaces the mass transport is dominant alongside the step edges. The analysis of the equilibrium fluctuations is consistent with the analysis of the decay of a non-equilibrium step profile. From the temperature dependence we have determined the averaged diffusion energy and an upper limit for the hopping barrier of adatoms along a (100) step. We have demonstrated that the analysis of the time dependence of step fluctuations in equilibrium and of the time dependence of a bump decay yields consistent quantitative results. For higher temperatures we find indications for a transition to a mass transport which involves mass exchange with the terraces. Careful measurements of the time dependence for different tunneling parameters prove that there is no measurable influence of the tunneling tip onto the data.

Acknowledgements

The authors gratefully acknowledge the skilful crystal preparation by Udo Linke. We appreciate helpful discussions with N.C. Bartelt and the critical reading of the manuscript by H. Ibach. This work was partially supported by the Fond der Chemischen Industrie, Germany.

References

[1] N.C. Bartelt, J.L. Goldberg, T.L. Einstein, E.D. Williams, J.C. Heyraud, J.J. Métois, Phys. Rev. B 48 (1993) 15453.
[2] L. Kuipers, M.S. Hoogeman, J.W.M. Frenken, Phys. Rev. Lett. 71 (1993) 3517.
[3] M. Giesen-Seibert, R. Jentjens, M. Poensgen, H. Ibach, Phys. Rev. Lett. 71 (1993) 3521.
[4] M. Giesen-Seibert, R. Jentjens, M. Poensgen, H. Ibach, Phys. Rev. Lett. 73 (1994) E911.
[5] M. Giesen-Seibert, H. Ibach, Surf. Sci. 316 (1994) 205.
[6] M. Giesen-Seibert, F. Schmitz, R. Jentjens, H. Ibach, Surf. Sci. 329 (1995) 47.
[7] L. Masson, L. Barbier, J. Cousty, Surf. Sci. 317 (1994) L1115.
[8] L. Kuipers, M.S. Hoogeman, H. van Beijeren, Phys. Rev. B 52 (1995) 11387.
[9] W.W. Pai, N.C. Bartelt, J.E. Reutt-Robey, Phys. Rev. B 53 (1996) 15991.
[10] L. Barbier, L. Masson, B. Salanon, Surf. Sci. 345 (1996) 197.
[11] M. Giesen, G. Schulze Icking-Konert, D. Stapel, H. Ibach, Surf. Sci. 366 (1996) 229.
[12] M. Giesen, M. Dietterle, D. Stapel, H. Ibach, D.M. Kolb, Surf. Sci. 384 (1997) 168.
[13] K. Morgenstern, G. Rosenfeld, E. Lægsgaard, F. Besenbacher, G. Comsa, Phys. Rev. Lett. 80 (1998) 556.

[14] K. Morgenstern, G. Rosenfeld, G. Comsa, Phys. Rev. Lett. 76 (1996) 2113.
[15] N.C. Bartelt, W. Theis, R.M. Tromp, Phys. Rev. B 54 (1996) 11741.
[16] J.B. Hannon, C. Klünker, M. Giesen, H. Ibach, N.C. Bartelt, J.C. Hamilton, Phys. Rev. Lett. 79 (1997) 2506.
[17] M. Giesen, G. Schulze Icking-Konert, H. Ibach, Phys. Rev. Lett. 80 (1998) 552.
[18] G. Schulze Icking-Konert, M. Giesen, H. Ibach, Surf. Sci. 398 (1998) 37.
[19] J. Li, R. Berndt, W.-D. Schneider, Phys. Rev. Lett. 76 (1996) 1888.
[20] F. Mugele, A. Rettenberger, J. Boneberg, P. Leiderer, Surf. Sci. 400 (1998) 80.
[21] F. Mugele, A. Rettenberger, J. Boneberg, P. Leiderer, Surf. Sci. 377–379 (1997) 62.
[22] W.W. Mullins, in: W.D. Robertson, N.A. Gjostein (Eds.), Metal Surfaces, American Society for Metals, Metals Park, OH, 1962.
[23] A. Pimipinelli, J. Villain, D.E. Wolf, J.J. Métois, J.C. Heyraud, I. Elkinani, G. Uimin, Surf. Sci. 295 (1993) 143.
[24] N.C. Bartelt, J.L. Goldberg, T.L. Einstein, E.D. Williams, Surf. Sci. 273 (1992) 252.
[25] N.C. Bartelt, T.L. Einstein, E.D. Williams, Surf. Sci. 240 (1990) L591.
[26] N.C. Bartelt, T.L. Einstein, E.D. Williams, Surf. Sci. 312 (1994) 411.
[27] M. Poensgen, J.F. Wolf, J. Frohn, M. Giesen, H. Ibach, Surf. Sci. 274 (1992) 430.
[28] B. Loisel, D. Gorse, V. Pontikis, J. Lapujoulade, Surf. Sci. 221 (1989) 365.
[29] P. Stoltze, J. Phys. Condens. Matter 6 (1994) 9495.
[30] G.L. Kellogg, Surf. Sci. Rep. 21 (1994) 1.
[31] A. Natori, R.W. Godby, Phys. Rev. B 47 (1993) 15816.
[32] M. Giesen, G. Schulze Icking-Konert, D. Stapel, H. Ibach, Surf. Sci. 366 (1996) 229.
[33] N.C. Bartelt, R.M. Tromp, Phys. Rev. B 54 (1996) 11731.